SIAM J. SCI. COMPUT.
Vol. 31, No. 5, pp. 3959–3978
© 2009 Society for Industrial and Applied Mathematics

# AN ITERATIVE METHOD FOR THE STOKES-TYPE PROBLEM WITH VARIABLE VISCOSITY*

PIOTR P. GRINEVICH† AND MAXIM A. OLSHANSKII†

**Abstract.** This paper concerns an iterative technique for solving discretized Stokes-type equations with varying viscosity coefficient. We build a special block preconditioner for the discrete system of equations and perform an analysis revealing its properties; the theoretical analysis is based on the weighted Nečas inequality. The subject of this paper is motivated by numerical solution of incompressible non-Newtonian fluid equations. In particular, the general analysis is applied to the linearized equations of the regularized Bingham model of viscoplastic fluid. Numerical experiments show that the suggested preconditioner leads to an iterative method insensitive to the variation of mesh size and the regularization parameter of the fluid model.

**Key words.** iterative methods, saddle-point problem, varying viscosity, weighted Nečas inequality, non-Newtonian fluid, Bingham fluid

**AMS subject classifications.** 65N06, 65N12, 74C10, 76D07

**DOI.** 10.1137/08744803

## 1. Introduction.

Certain mathematical models involve flow equations with nonconstant viscosity coefficient. This occurs, for example, in geophysical and convection flows, when the viscosity is a function of the temperature (see, e.g., [8, 35]), or in turbulence modeling [37]. Another example is non-Newtonian fluids modeling, when the Cauchy stress tensor is given by $\boldsymbol{\sigma} = 2\nu(|\mathbf{Du}|, p)\mathbf{Du} - p\,\mathbf{I}$, where $p$ is the pressure; $\mathbf{Du} = \frac{1}{2}(\nabla\mathbf{u} + \nabla^T\mathbf{u})$ is the rate of the deformation tensor; $\mathbf{u}$ denotes the velocity; and $\nu(\cdot)$ is the viscosity which may depend on the second invariant of the rate deformation tensor $|\mathbf{Du}| = \left(\frac{1}{2}\mathrm{tr}([\mathbf{Du}]^2)\right)^{\frac{1}{2}}$ and the pressure. Depending on the specific viscosity function $\nu(\cdot)$, this setting includes the following models (with appropriate parameters $\nu_0, r, \tau_s$): non-Newtonian flow due to power law, with $\nu(|\mathbf{Du}|, p) = \nu_0 + \tau_s|\mathbf{Du}|^{r-2}$, e.g., the Bingham model with $r = 1$, and non-Newtonian flow with pressure and shear-dependent viscosity, as considered for instance in [17, 21, 29]. Often a regularization is introduced in a model to avoid the singularity of $\nu$ for $|\mathbf{Du}| = 0$, as described in section 4 for the Bingham model. Newtonian flow is represented by $\nu(\cdot) = \nu_0$.

In all cases, the velocity $\mathbf{u}$ and the pressure $p$ satisfy the following generalized Navier–Stokes equations:

$$\frac{\partial \mathbf{u}}{\partial t} + \mathbf{u}\cdot\nabla\mathbf{u} - \mathbf{div}\nu(|\mathbf{Du}|, p)\mathbf{Du} + \nabla p = \mathbf{g}, \quad \text{div } \mathbf{u} = \mathbf{0}. \tag{1.1}$$

We assume that equations (1.1) hold in the whole computational domain $\Omega \subset \mathbb{R}^d$, $d = 2, 3$. This may require a regularization for the case of $\nu \to \infty$. Further, we consider a steady flow and neglect the inertia terms. In Remark 6 we discuss how the results of the paper can be extended for the case of unsteady flows and if the inertia

*Received by the editors December 23, 2008; accepted for publication (in revised form) August 21, 2009; published electronically November 5, 2009. This work was supported by the German Research Foundation and the Russian Foundation for Basic Research through projects 09-01-00115 and 08-01-00159.

http://www.siam.org/journals/sisc/31-5/74480.html

†Department of Mechanics and Mathematics, Moscow State M.V. Lomonosov University, Moscow 119899, Russia (p.grinevich@gmail.com, Maxim.Olshanskii@mtu-net.ru).



Copyright © by SIAM. Unauthorized reproduction of this article is prohibited.

terms are taken into account. The resulting system of equations can be written in the form

$$F(\mathbf{u},p)\circ\begin{pmatrix}\mathbf{u}\\ p\end{pmatrix}=\begin{pmatrix}\mathbf{g}\\ 0\end{pmatrix}, \tag{1.2}$$

with the *linear* operator (for a fixed vector function $\mathbf{a}$ and scalar function $\xi$) of the following $2\times 2$ block form:

$$F(\mathbf{a},\xi):=\begin{pmatrix}-\mathbf{div}\,\nu(|\mathbf{D}\mathbf{a}|,\xi)\mathbf{D} & \nabla\\ -\mathrm{div} & 0\end{pmatrix}. \tag{1.3}$$

For simplicity, we pose the Dirichlet boundary conditions for velocity:

$$\mathbf{u}=\mathbf{u}_b \quad \text{on} \quad \partial\Omega. \tag{1.4}$$

The vector function $\mathbf{u}_b$ satisfies $\int_{\partial\Omega}\mathbf{u}_b\cdot\mathbf{n}=0$. We solve (1.2), (1.4) with the Picard iterative method (we also discuss the application of the Newton method in section 5.3):

$$\begin{pmatrix}\mathbf{u}^n\\ p^n\end{pmatrix}=\begin{pmatrix}\mathbf{u}^{n-1}\\ p^{n-1}\end{pmatrix}-\widetilde{F}(\mathbf{u}^{n-1},p^{n-1})^{-1}\circ\left[F(\mathbf{u}^{n-1},p^{n-1})\circ\begin{pmatrix}\mathbf{u}^{n-1}\\ p^{n-1}\end{pmatrix}-\begin{pmatrix}\mathbf{g}\\ 0\end{pmatrix}\right]. \tag{1.5}$$

Here $\widetilde{F}(\mathbf{u}^{n-1},p^{n-1})^{-1}$ is an *approximate* solution to the linear problem

$$F(\mathbf{u}^{n-1},p^{n-1})\circ\begin{pmatrix}\mathbf{v}\\ q\end{pmatrix}=\begin{pmatrix}\mathbf{f}\\ g\end{pmatrix} \quad \text{with} \quad \mathbf{v}=0 \ \text{ on } \ \partial\Omega, \tag{1.6}$$

where $\mathbf{f}$ and $g$ denote corresponding residuals from (1.5) in momentum and continuity equations, respectively. Given $\mathbf{u}^{n-1}$ and $p^{n-1}$, problem (1.6) can be written as the Stokes-type problem with the variable viscosity coefficient $\nu(\mathbf{x}):=\nu(|\mathbf{D}\mathbf{u}^{n-1}|,p^{n-1})$:

$$\begin{aligned}-\mathbf{div}\nu(\mathbf{x})\mathbf{D}\mathbf{v}+\nabla q&=\mathbf{f} \quad \text{on} \quad \Omega,\\ -\mathrm{div}\ \mathbf{v}&=g \quad \text{on} \quad \Omega,\\ \mathbf{v}&=0 \quad \text{on} \quad \partial\Omega.\end{aligned} \tag{1.7}$$

Obviously, solving (1.7) is the most computationally consuming step in the entire approach. Of course, in practice, (1.5) is applied to the system of *discretized* equations. Thus the main concern of the paper is the development and analysis of preconditioned iterative methods for solving the discrete counterpart of (1.7).

The rest of the paper is organized as follows. In section 2 we consider a general iterative approach for solving (1.7) and in section 3 we discuss and analyze some choices of preconditioner. In section 4 the analysis is applied to the particular case of the regularized Bingham model of non-Newtonian fluid. Section 5 collects the results of numerical experiments for two model problems of the Bingham fluid flows discretized with finite element (FE) and finite difference (FD) methods.

**2. Linear solver.** In this section we deal with a discrete counterpart of (1.7). Here and in the remainder of the paper, the $L^2$ scalar product and associated norm are denoted by $(\cdot,\cdot)$ and $\|\cdot\|$, respectively. Moreover, we will simply use the notation $\nu$ for the variable viscosity coefficient. To define the pressure space uniquely,

Copyright © by SIAM. Unauthorized reproduction of this article is prohibited.

some factorization of $L^2(\Omega)$ is introduced. In this paper we will use two different factorizations:

$$L_0^2(\Omega) := \{q \in L^2(\Omega) \mid (q,1) = 0\} \quad \text{and} \quad L_\nu^2(\Omega) := \{q \in L^2(\Omega) \mid (q,\nu^{-1}) = 0\}.$$

To fix ideas, let us consider FE spaces for velocity $\mathbb{V}_h \subset \mathbf{H}_0^1(\Omega)$ and pressure $\mathbb{Q}_h \subset L_0^2(\Omega)$. Assume that the pair of spaces $\mathbb{V}_h$, $\mathbb{Q}_h$ is stable in the LBB sense (see, e.g., [5]); i.e., there exists a mesh-independent constant $c_0 > 0$ such that

$$c_0 \le \inf_{q_h \in \mathbb{Q}_h} \sup_{\mathbf{v}_h \in \mathbb{V}_h} \frac{(q_h, \operatorname{div} \mathbf{v}_h)}{\|q_h\| \, \|\nabla \mathbf{v}_h\|}. \tag{2.1}$$

Here and in what follows we always take $\inf_x$ or $\sup_x$ over nonzero elements if $\|x\|$ appears in the denominator. The FE discretization of (1.7) consists of finding $\mathbf{u}_h \in \mathbb{V}_h$ and $p_h \in \mathbb{Q}_h$ such that

$$(\nu \mathbf{D}\mathbf{u}_h, \mathbf{D}\mathbf{v}_h) - (p_h, \operatorname{div} \mathbf{v}_h) - (q_h, \operatorname{div} \mathbf{u}_h) = (\mathbf{f}_h, \mathbf{v}_h) + (g_h, q_h) \quad \forall\, \mathbf{v}_h \in \mathbb{V}_h,\ q_h \in \mathbb{Q}_h. \tag{2.2}$$

Let $\{\phi_i\}_{1 \le i \le n}$ and $\{\psi_j\}_{1 \le j \le m}$ be nodal bases of $\mathbb{V}_h$ and $\mathbb{Q}_h$, respectively. Define the matrices $A = \{A_{i,j}\} \in \mathbb{R}^{n \times n}$, $B = \{B_{i,j}\} \in \mathbb{R}^{m \times n}$, and $M = \{M_{i,j}\} \in \mathbb{R}^{m \times m}$ with

$$A_{i,j} = (\nu \mathbf{D}\phi_j, \mathbf{D}\phi_i), \quad B_{i,j} = -(\operatorname{div} \phi_j, \psi_i), \quad M_{i,j} = (\psi_j, \psi_i).$$

The linear algebraic system corresponding to (2.2) takes the form

$$\begin{pmatrix} A & B^T \\ B & 0 \end{pmatrix} \begin{pmatrix} u \\ p \end{pmatrix} = \begin{pmatrix} f \\ g \end{pmatrix}. \tag{2.3}$$

We are interested in solving (2.3) by a preconditioned iterative method. Following [33], we consider the block diagonal preconditioner for the system (2.3):

$$\mathcal{P} = \begin{pmatrix} \widehat{A} & 0 \\ 0 & -\widehat{S} \end{pmatrix}. \tag{2.4}$$

The matrix $\widehat{A}$ is a preconditioner for the matrix $A$, such that $\widehat{A}^{-1}$ may be considered as an inexact solver for linear systems involving $A$. The matrix $\widehat{S}$ is a preconditioner for the pressure Schur complement of (2.3), $S = BA^{-1}B^T$. In an iterative algorithm one needs the actions of $\widehat{A}^{-1}$ and $\widehat{S}^{-1}$ on subvectors, rather than the matrices $\widehat{A}$, $\widehat{S}$ explicitly. Once good preconditioners for $A$ and $S$ are given, an appropriate Krylov subspace iterative method for (2.3) (such as MINRES [32] with the block preconditioner (2.4)) is an efficient solver.

Given preconditioners $\widehat{A}^{-1}$ and $\widehat{S}^{-1}$, one has the choice of several other iterative techniques for solving problem (2.3), including a preconditioned conjugate gradient method through a special transformation of (2.3) [4] and an inexact Uzawa-type method [1]; see also the review paper [2]. As an option we also use the approach well suited for more general nonsymmetric problems (see Remark 6) of the same structure [12]—the BiCGstab iterative method with the block triangular preconditioner:

$$\mathcal{P}_1 = \begin{pmatrix} \widehat{A} & 0 \\ B & -\widehat{S} \end{pmatrix}. \tag{2.5}$$

Copyright © by SIAM. Unauthorized reproduction of this article is prohibited.

In the literature one can find geometric or algebraic multigrid (see, e.g., [16, 34, 25]) or domain decomposition [31] iterative algorithms which provide effective preconditioners $\widehat{A}$ if the function $\nu$ is sufficiently regular; see, however, Remark 5. At the same time, building a preconditioner for $S$ is a more delicate issue, since $S$ is given *implicitly* and $S$ is *not* a sparse matrix. In the next section we analyze two preconditioners for $S$.

**3. Schur complement preconditioning.** The matrix $S$ has one dimensional kernel, corresponding to the constant pressure mode. Further, we will consider $S$ as an invertible operator on an appropriate subspace.[1] Thus, when it does not cause confusion, we treat $S$ as a nonsingular matrix. For the Stokes problem it is well known that $S$ is spectrally equivalent to the pressure mass matrix $M$. The lemma below extends the result to the case of the variable viscosity coefficient and the rate of deformation tensor formulation. For two matrices $A$ and $B$ we write $A \geq B$ if $A - B$ is semipositive definite. We will use the notation $\langle \cdot, \cdot \rangle$ for the Euclidean scalar product.

Denote

$$\nu_{\min} = \inf_{\Omega} \nu(\mathbf{x}), \qquad \nu_{\max} = \sup_{\Omega} \nu(\mathbf{x}).$$

The natural assumption is that $\nu_{\min} > 0$ and $\nu_{\max} < \infty$.

LEMMA 3.1. *Assume* (2.1)*; then it holds that*

$$c_0^2 \nu_{\max}^{-1} M \leq S \leq \nu_{\min}^{-1} M. \tag{3.1}$$

*Proof.* For arbitrary pressure FE function $q_h \in \mathbb{Q}_h$, denote by $q$ the corresponding vector of coefficients from $\mathbb{R}^m$. Due to the definitions of matrices $A$, $B$, and $M$, it holds that

$$\langle S\, q, q \rangle = \langle A^{-1} B^T q, B^T q \rangle = \sup_{v \in \mathbb{R}^n} \frac{\langle v, B^T q \rangle^2}{\langle A\, v, v \rangle} = \sup_{\mathbf{v}_h \in \mathbb{V}_h} \frac{(q_h, \operatorname{div} \mathbf{v}_h)^2}{\|\nu^{\frac{1}{2}} \mathbf{D} \mathbf{v}_h\|^2}, \tag{3.2}$$

$$\langle M\, q, q \rangle = \|q_h\|^2. \tag{3.3}$$

Note that due to the identities $\operatorname{rot}^2 + \nabla \operatorname{div} = \Delta = 2\mathbf{div}\mathbf{D} - \nabla \operatorname{div}$ it holds that (one can apply integration by parts to verify)

$$\|\operatorname{rot} \mathbf{v}\|^2 + \|\operatorname{div} \mathbf{v}\|^2 = \|\nabla \mathbf{v}\|^2 = 2\|\mathbf{D}\mathbf{v}\|^2 - \|\operatorname{div} \mathbf{v}\|^2 \qquad \forall\ \mathbf{v} \in \mathbf{H}_0^1(\Omega).$$

Hence

$$\|\operatorname{div} \mathbf{v}\|^2 \leq \|\mathbf{D}\mathbf{v}\|^2 \leq \|\nabla \mathbf{v}\|^2 \qquad \forall\ \mathbf{v} \in \mathbf{H}_0^1(\Omega). \tag{3.4}$$

Using estimates (3.4) and embedding $\mathbb{V}_h \subset \mathbf{H}_0^1(\Omega)$ and the Cauchy inequality we get

$$\|\nu^{\frac{1}{2}} \mathbf{D} \mathbf{v}_h\|^2 \leq \nu_{\max} \|\mathbf{D}\mathbf{v}_h\|^2 \leq \nu_{\max} \|\nabla \mathbf{v}_h\|^2 \tag{3.5}$$

and

$$(q_h, \operatorname{div} \mathbf{v}_h) \leq \|q_h\| \|\operatorname{div} \mathbf{v}_h\| \leq \|q_h\| \|\mathbf{D}\mathbf{v}_h\| \leq \nu_{\min}^{-\frac{1}{2}} \|q_h\| \|\nu^{\frac{1}{2}} \mathbf{D} \mathbf{v}_h\|. \tag{3.6}$$

[1] This $(m-1)$-dimensional subspace can be characterized as all $q \in \mathbb{R}^m$ such that $q_h \in \mathbb{Q}_h$, where $q$ is the vector of (nodal) coefficients for $q_h$.

Copyright © by SIAM. Unauthorized reproduction of this article is prohibited.

Relations (3.2), (3.3), together with estimates (3.5)–(3.6) and (2.1) yield

$$c_0^2 \nu_{\max}^{-1} \langle M\, q, q\rangle \le \langle S\, q, q\rangle \le \nu_{\min}^{-1} \langle M\, q, q\rangle.$$

Thus the lemma is proved. ∎

From the result of the lemma it follows that

$$\operatorname{cond}(\widehat{S}^{-1} S) \le c_0^{-2} \frac{\nu_{\max}}{\nu_{\min}} \qquad \text{with} \quad \widehat{S} = M. \tag{3.7}$$

Since $M^{-1}$ is not a sparse matrix, it is a common approach to use, instead of $M$, a diagonal approximation $\widehat{M} = \operatorname{diag}(M)$ as a preconditioner for $S$. For a family of grids satisfying the minimal angle condition it holds [39] that $c_m \widehat{M} \le M \le C_m \widehat{M}$ with positive mesh-independent constants $c_m$ and $C_m$. Therefore, an estimate similar to (3.7) holds with $M$ replaced by $\widehat{M}$. In either case the resulting preconditioner becomes inefficient for problems with the large ratio $\nu_{\max}/\nu_{\min}$. Since in a particular application of our interest it often holds that $\nu_{\max}/\nu_{\min} \gg 1$, we suggest a new preconditioner below, which accounts for the variable coefficient $\nu$. To this end, define the following mass type matrix $M_\nu = \{(M_\nu)_{i,j}\} \in \mathbb{R}^{m\times m}$ with

$$(M_\nu)_{i,j} = (\nu^{-1}\psi_j, \psi_i). \tag{3.8}$$

In the remainder of this section we assume $\mathbb{Q}_h \subset L^2_\nu$. In [27] it was proved that for the case of *piecewise constant*

$$\nu(\mathbf{x}) = \begin{cases} \nu_1, & \mathbf{x} \in \Omega_1, \\ \nu_2, & \mathbf{x} \in \Omega \setminus \Omega_1, \end{cases}$$

the inequalities

$$c_\nu M_\nu \le S \le C_\nu M_\nu \tag{3.9}$$

hold with constants $c_\nu > 0$ and $C_\nu$ independent of mesh size and the values of $\nu_1 > 0$ and $\nu_2 > 0$ ($c_\nu$ and $C_\nu$ depend, however, on $\Omega_1$). This observation as well as the simple scaling argument $S \to \lambda^{-1} S$ if $\nu \to \lambda\nu$, lead us to the choice of $M_\nu$ as a preconditioner to $S$. One can easily prove the following result.

LEMMA 3.2. *For a positive $\nu \in L^\infty(\Omega)$ and $\Omega \subset \mathbb{R}^d$, the upper bound in* (3.9) *holds with $C_\nu = d$.*

*Proof.* By direct computation we verify the inequality $\|\nu^{\frac12} \operatorname{div} \mathbf{v}\| \le \sqrt{d}\|\nu^{\frac12}\mathbf{D}\mathbf{v}\|$ for any $\mathbf{v} \in \mathbf{H}^1_0(\Omega)$. This and the Cauchy inequality give

$$\sup_{\mathbf{v}_h \in \mathbb{V}_h} \frac{(q_h, \operatorname{div}\mathbf{v}_h)^2}{\|\nu^{\frac12}\mathbf{D}\mathbf{v}_h\|^2} \le \sup_{\mathbf{v}_h \in \mathbb{V}_h} \frac{\|\nu^{-\frac12} q_h\|^2 \|\nu^{\frac12}\operatorname{div}\mathbf{v}_h\|^2}{\|\nu^{\frac12}\mathbf{D}\mathbf{v}_h\|^2} \le d\|\nu^{-\frac12} q_h\|^2 = d\langle M_\nu\, q, q\rangle \tag{3.10}$$

for any $q_h \in \mathbb{Q}_h$ and the corresponding vector of coefficients $q$. Now the results in (3.2) and (3.10) prove the lemma. ∎

Using arguments similar to the proof of Lemma 3.1, it is easy to show that the constant $c_\nu$ in (3.9) can be taken as $c_\nu = c_0^2 \nu_{\min} \nu_{\max}^{-1}$. This bound for $c_\nu$ leads to the estimate of $\operatorname{cond}(M_\nu^{-1} S)$ similar to (3.7). However, numerical experiments (see section 5.1) show that for particular coefficients $\nu$ appearing in non-Newtonian flow calculations, the effective condition number of $M_\nu^{-1} S$ is uniformly bounded with respect to $\nu_{\min}\nu_{\max}^{-1}$. The same experiments show that the result in (3.7) is sharp. To

Copyright © by SIAM. Unauthorized reproduction of this article is prohibited.

gain a better insight into the properties of the $\nu$-dependent preconditioning, we consider the "continuous" setting of the problem; i.e., instead of FE spaces and operators we consider the original differential ones. In such a setting the lower bound in (3.9) is equivalent to the following estimate (cf. (3.2), (3.8)) for any $q \in L^2_\nu(\Omega)$:

$$\tilde{c}_\nu \|\nu^{-\frac{1}{2}} q\|^2 \le \sup_{\mathbf{v}\in\mathbf{H}^1_0(\Omega)} \frac{(q, \operatorname{div}\mathbf{v})^2}{\|\nu^{\frac{1}{2}}\mathbf{D}\mathbf{v}\|^2}, \tag{3.11}$$

with $\tilde{c}_\nu > 0$. For $\nu \equiv 1$, (3.11) is equivalent to the *Nečas inequality* [20, 24] (the continuous counterpart of the LBB condition (2.1)). Thus (3.11) can be observed as the weighted Nečas inequality. First we prove the following lemma.

LEMMA 3.3. *Assume that $\nu$ is sufficiently smooth, so the norms below make sense. Then* (3.11) *holds for any $q \in L^2_\nu(\Omega)$ such that $(q, \nu^{-\frac{1}{2}}) = 0$ with the constant $\tilde{c}_\nu$ defined below. If $d = 2$, then*

$$\tilde{c}_\nu = \tilde{c}_0 (1 + c(k,r)\, \|\nu^{\frac{1}{2}}\|_{L^k} \|\nabla \nu^{-\frac{1}{2}}\|_{L^r})^{-2} \tag{3.12}$$

*with any $k > 2$ and $r > \frac{2k}{k-2}$. Here $c(k,r)$ depends on constants from embedding inequalities of $H^1_0(\Omega)$ into $L^t(\Omega)$ with $t = t(k,r)$, and $\tilde{c}_0$ depends only on the constant from the Nečas inequality. If $d = 3$, then*

$$\tilde{c}_\nu = \tilde{c}_0 (1 + c\, \|\nu^{\frac{1}{2}}\|_{L^k} \|\nabla \nu^{-\frac{1}{2}}\|_{L^r})^{-2} \tag{3.13}$$

*with any $k > 3$ and $r = \frac{3k}{k-3}$.*

*Proof.* The Nečas inequality is equivalent to the following result: for any $r \in L^2_0(\Omega)$ there exists $\mathbf{w} \in \mathbf{H}^1_0(\Omega)$ such that

$$\operatorname{div}\mathbf{w} = r \qquad \text{and} \qquad \|\nabla \mathbf{w}\| \le C\, \|r\| \tag{3.14}$$

with a constant $C$ depending only on $\Omega$. For an arbitrary $q \in L^2_\nu(\Omega)$ satisfying $(q, \nu^{-\frac{1}{2}}) = 0$, consider $\mathbf{w}$ given by (3.14) for $r = \nu^{-\frac{1}{2}} q \in L^2_0(\Omega)$. Observe the identity

$$\operatorname{div}(\nu^{-\frac{1}{2}}\mathbf{w}) = \nu^{-\frac{1}{2}} \operatorname{div}\mathbf{w} + \mathbf{w}\cdot\nabla\nu^{-\frac{1}{2}}. \tag{3.15}$$

Note that $(\nu^{-\frac{1}{2}} \operatorname{div}\mathbf{w}, 1) = (\nu^{-1} q, 1) = 0$ and $(\operatorname{div}(\nu^{-\frac{1}{2}}\mathbf{w}), 1) = (\nu^{-\frac{1}{2}}\mathbf{w}, \nabla 1) = 0$; due to (3.15), this yields $(\mathbf{w}\cdot\nabla\nu^{-\frac{1}{2}}, 1) = 0$. Therefore, we may define $\mathbf{u} \in \mathbf{H}^1_0(\Omega)$ solving the following Stokes problem:

$$\begin{aligned} -\Delta\mathbf{u} + \nabla\xi = 0, \quad \operatorname{div}\mathbf{u} = \mathbf{w}\cdot\nabla\nu^{-\frac{1}{2}} \quad &\text{on} \quad \Omega, \\ \mathbf{u} = 0 \quad &\text{on} \quad \partial\Omega. \end{aligned}$$

One has the following a priori estimate for the solution of the Stokes problem [36]:

$$\|\nabla\mathbf{u}\|_{L^s} \le C\, \|\mathbf{w}\cdot\nabla\nu^{-\frac{1}{2}}\|_{L^s} \qquad \forall\ s > 1. \tag{3.16}$$

Now we set $\mathbf{v} = \nu^{-\frac{1}{2}}\mathbf{w} - \mathbf{u}$. Thanks to (3.14) and (3.15), it holds that

$$(\operatorname{div}\mathbf{v}, q) = (\operatorname{div}\mathbf{w}, \nu^{-\frac{1}{2}} q) = \|\nu^{-\frac{1}{2}} q\|^2. \tag{3.17}$$

It remains to estimate $\|\nu^{\frac{1}{2}}\mathbf{D}\mathbf{v}\|$. We have

$$\|\nu^{\frac{1}{2}}\mathbf{D}\mathbf{v}\| \le c\|\nu^{\frac{1}{2}}\nabla\mathbf{v}\| \le c(\|\nu^{\frac{1}{2}}\nabla(\nu^{-\frac{1}{2}}\mathbf{w})\| + \|\nu^{\frac{1}{2}}\nabla\mathbf{u}\|). \tag{3.18}$$

Copyright © by SIAM. Unauthorized reproduction of this article is prohibited.

We now assume $d = 2$ and we estimate the terms on the right-hand side of (3.18) separately. Using Hölder's inequality and the embedding inequality $\|\mathbf{w}\|_{L^r} \le c(r)\|\nabla \mathbf{w}\|$ for all $r \in [1, \infty)$, we get

$$\begin{aligned}(3.19)\qquad \|\nu^{\frac{1}{2}}\nabla(\nu^{-\frac{1}{2}}\mathbf{w})\| &\le \|\nabla \mathbf{w}\| + \|\nu^{\frac{1}{2}}\mathbf{w}\cdot\nabla\nu^{-\frac{1}{2}}\| \\ &\le \|\nabla \mathbf{w}\| + \|\nu^{\frac{1}{2}}\nabla\nu^{-\frac{1}{2}}\|_{L^{2k}}\|\mathbf{w}\|_{L^{2r}} \\ &\le (1 + c(k)\|\nu^{\frac{1}{2}}\nabla\nu^{-\frac{1}{2}}\|_{L^{2k}})\|\nabla \mathbf{w}\| \qquad \forall\ k > 1,\ r = \tfrac{k}{k-1}.\end{aligned}$$

Using Hölder's inequality and embedding inequalities and (3.16), we estimate the second term as

$$\begin{aligned}(3.20)\qquad \|\nu^{\frac{1}{2}}\nabla \mathbf{u}\| &\le \|\nu^{\frac{1}{2}}\|_{L^{2k}}\|\nabla \mathbf{u}\|_{L^{2r}} \le c\,\|\nu^{\frac{1}{2}}\|_{L^{2k}}\|\mathbf{w}\cdot\nabla\nu^{-\frac{1}{2}}\|_{L^{2r}} \\ &\le c(s)\,\|\nu^{\frac{1}{2}}\|_{L^{2k}}\|\nabla\nu^{-\frac{1}{2}}\|_{L^{2r+s}}\|\nabla \mathbf{w}\| \qquad \forall\ k > 1,\ s > 0,\ r = \tfrac{k}{k-1}.\end{aligned}$$

Note that Hölder's inequality gives $\|\nu^{\frac{1}{2}}\nabla\nu^{-\frac{1}{2}}\|_{L^{2k}} \le \|\nu^{\frac{1}{2}}\|_{L^{\ell}}\|\nabla\nu^{-\frac{1}{2}}\|_{L^{2k\ell/(\ell-2k)}}$ for any $\ell > 2k$. For any $s > 0$ we take $k$ sufficiently close to 1 to ensure $2k\ell/(\ell - 2k) \le 2\ell/(\ell-2) + s$. Therefore, from (3.18)–(3.20) and (3.14), with $r = \nu^{-\frac{1}{2}}q$, we obtain

$$(3.21)\qquad \|\nu^{\frac{1}{2}}\mathbf{D}\mathbf{v}\| \le c\,(1 + c(s)\,\|\nu^{\frac{1}{2}}\|_{L^{\ell}}\|\nabla\nu^{-\frac{1}{2}}\|_{L^{r+s}})\|\nu^{-\frac{1}{2}}q\|$$

with any $\ell > 2$, $s > 0$, and $r = \frac{2\ell}{\ell-2}$. Relations (3.17) and (3.21) yield (3.11) with $\tilde{c}_\nu$ as in (3.12).

We now assume $d = 3$. In this case, it holds that $\|\mathbf{w}\|_{L^6} \le c\,\|\nabla \mathbf{w}\|$. With the same arguments as in (3.19)–(3.21) we get

$$(3.22)\qquad \|\nu^{\frac{1}{2}}\nabla(\nu^{-\frac{1}{2}}\mathbf{w})\| \le (1 + c\,\|\nu^{\frac{1}{2}}\nabla\nu^{-\frac{1}{2}}\|_{L^3})\|\nabla \mathbf{w}\|$$

and

$$(3.23)\qquad \|\nu^{\frac{1}{2}}\nabla \mathbf{u}\| \le c\,\|\nu^{\frac{1}{2}}\|_{L^{2k}}\|\nabla\nu^{-\frac{1}{2}}\|_{L^{2r}}\|\nabla \mathbf{w}\| \qquad \forall\ k \ge \tfrac{3}{2},\ r = \tfrac{3k}{2k-3}.$$

Hölder's inequality gives $\|\nu^{\frac{1}{2}}\nabla\nu^{-\frac{1}{2}}\|_{L^3} \le \|\nu^{\frac{1}{2}}\|_{L^{3k}}\|\nabla\nu^{-\frac{1}{2}}\|_{L^{3k/(k-1)}}$. Therefore, it holds that

$$(3.24)\qquad \|\nu^{\frac{1}{2}}\mathbf{D}\mathbf{v}\| \le c\,(1 + c\,\|\nu^{\frac{1}{2}}\|_{L^{k}}\|\nabla\nu^{-\frac{1}{2}}\|_{L^{r}})\|\nu^{-\frac{1}{2}}q\|$$

with any $k > 3$ and $r = \frac{3k}{k-3}$. Relations (3.17) and (3.24) yield (3.11) with $\tilde{c}_\nu$ as in (3.13). ∎

*Remark* 1. Define two linear continuous functionals on $L^2(\Omega)$: $f_1(q) := (q, \nu^{-1})$ and $f_2(q) := (q, \nu^{-\frac{1}{2}})$. Lemma 3.3 provides a bound in (3.11) on $H := (\ker(f_1) \cup \ker(f_2))^{\perp}$. If $\nu \ne \text{const}$, then $\dim(\ker(f_1) \cup \ker(f_2)) = 2$ and $\dim(H) = \infty$. For $\nu = \text{const}$, both constraints from Lemma 3.3 are equivalent to $(q, 1) = 0$, which is consistent with the well-known (nonweighted) Nečas inequality.

Estimates (3.12)–(3.13) can be more useful than the trivial one ($\tilde{c}_\nu \ge c_0^2\nu_{\min}\nu_{\max}^{-1}$) since they involve integral norms of $\nu$. However, from the example of the Bingham fluid, we will see that one may encounter situations when (3.12)–(3.13) do not lead to a significant improvement over the trivial estimate. At the same time, a (natural) partitioning of $\Omega$ into few subdomains $\Omega_i$ gives for the $\nu$-dependent terms in (3.12) and (3.13) the following:

$$(3.25)\qquad \sum_i \|\nu^{\frac{1}{2}}\|_{L^k(\Omega_i)}\|\nabla\nu^{-\frac{1}{2}}\|_{L^r(\Omega_i)} \ll \|\nu^{\frac{1}{2}}\|_{L^k(\Omega)}\|\nabla\nu^{-\frac{1}{2}}\|_{L^r(\Omega)}.$$

Copyright © by SIAM. Unauthorized reproduction of this article is prohibited.

By a domain decomposition argument, the result of Lemma 3.3 can be extended to provide useful bounds of $\tilde{c}_\nu$ in this case. Thus, we prove the following lemma.

LEMMA 3.4. *Let $\overline{\Omega} = \cup_{i=1}^N \overline{\Omega}_i$, where $\Omega_i$ are connected nonoverlapping subdomains with sufficiently regular boundary. Assume that $\nu$ is piecewise smooth with respect to this partitioning. Then, for any $q \in L^2(\Omega)$ such that $(q, \nu^{-\frac{1}{2}})_{L_2(\Omega_i)} = (q, \nu^{-1})_{L_2(\Omega_i)} = 0$ for $i = 1, \dots, N$, the inequality* (3.11) *holds with $\tilde{c}_\nu = \min_{1\le i\le N} \tilde{c}_\nu(\Omega_i)$, where $\tilde{c}_\nu(\Omega_i)$ is the constant given by* (3.12) *or* (3.13) *for the domain $\Omega_i$.*

*Proof.* Due to Lemma 3.3 in each $\Omega_i$ we can define $\mathbf{v}_i \in \mathbf{H}_0^1(\Omega_i)$ such that

$$(\operatorname{div} \mathbf{v}_i, q)_{L^2(\Omega_i)} = \|\nu^{-\frac{1}{2}} q\|^2_{L^2(\Omega_i)}, \qquad \tilde{c}_\nu(\Omega_i)^{\frac{1}{2}} \|\nu^{\frac{1}{2}} \mathbf{D}\mathbf{v}_i\|_{L^2(\Omega_i)} \le \|\nu^{-\frac{1}{2}} q\|_{L^2(\Omega_i)}.$$

For all $i$, we extend $\mathbf{v}_i$ by zero to the whole domain $\Omega$ and set $\mathbf{v} = \sum_{i=1}^N \mathbf{v}_i$. We get

$$(\operatorname{div} \mathbf{v}, q) = \|\nu^{-\frac{1}{2}} q\|^2, \qquad \min_{1\le i\le N} \tilde{c}_\nu(\Omega_i)^{\frac{1}{2}} \, \|\nu^{\frac{1}{2}} \mathbf{D}\mathbf{v}\| \le \|\nu^{-\frac{1}{2}} q\|. \qquad \square$$

*Remark* 2. The result in Lemma 3.4 requires $2N$ orthogonality conditions. These orthogonality conditions will be used solely in deducing bounds for eigenvalues of a preconditioned matrix (see the next remark), but never enter actual computations and an iterative algorithm.

*Remark* 3. Consider the eigenvalue problem

$$Sx = \lambda M_\nu x. \tag{3.26}$$

The corresponding eigenvalues $\lambda$ are real and the Courant–Fischer theorem gives for the $k$th eigenvalue the characterization

$$\lambda_k = \max_{\mathcal{K}\in\mathcal{V}_{k-1}} \min_{x\in\mathcal{K}^\perp} \frac{\langle Sx, x\rangle}{\langle M_\nu x, x\rangle}, \tag{3.27}$$

where $\mathcal{V}_{k-1}$ denotes the family of all $(k-1)$-dimensional subspaces of $\mathbb{R}^m$. If we *assume* that discrete counterparts of the estimate (3.11) and Lemma 3.4 are valid, then (3.27) immediately gives the following result. The eigenvalues of (3.26) satisfy

$$0 = \lambda_1 < \lambda_2 \le \lambda_3 \le \cdots \le \lambda_m \le d \quad \text{and} \quad \tilde{c}_\nu \le \lambda_{2N+1} \tag{3.28}$$

with $d = 2$ or $d = 3$.

Note that $2N - 1$ small eigenvalues would add at most $2N - 1$ extra iterations of a preconditioned Krylov subspace method like MINRES to converge with desired tolerance. Therefore, if the number of subdomains $N$ is small (this is the case in applications considered further), then the convergence rate is essentially determined by the value $\tilde{c}_\nu$. We also recall that the iterative method does not account for $\lambda_1 = 0$, since pressure approximations always belong to a proper subspace.

*Remark* 4. In iterative process (1.5) one may also define $\widetilde{F}(\mathbf{u}^{n-1}, p^{n-1})^{-1}$ as an approximate inverse of the Jacobian. This would lead to the inexact Newton method for (1.2). Although this approach leads potentially to quadratically convergent iterations, one has to choose a sufficiently good initial guess. Moreover, the (1,1)-block $A$ may not be positive definite anymore. For pressure-dependent viscosity, the linear system on each iteration loses the symmetric structure of (2.3), since the (2,1)-block is not adjoint to the (1,2)-block. This may lead to the loss of linear algebraic solvers' efficiency and makes a potential analysis even more involved. However, this inexact

Copyright © by SIAM. Unauthorized reproduction of this article is prohibited.

Newton approach is of interest and we will explore this option numerically for the regularized Bingham problem in section 5.3.

*Remark* 5. Standard analysis of optimal solvers such as multigrid methods for the discrete diffusion equation relies on bounds for the minima and some norms of the diffusion coefficient. Since such uniform bounds do not necessarily hold for $\nu(\mathbf{x})$, the application of these methods for solving or preconditioning the submatrix $A$ should be done with some care. Our numerical experience shows that a geometric multigrid method with ILU smoothings provides a fairly efficient preconditioner; results in [6] indicate that an AMG method may be a good option as well. Nevertheless, to separate the effect of preconditioning the submatrix $A$ from the effect of preconditioning the Schur complement matrix $S$, we use the exact factorization of $A$ for numerical experiments in this paper. The analysis of optimal preconditioning strategies for $A$ in conjunction with non-Newtonian fluid modeling is not a subject of the present paper.

*Remark* 6. If the inertia terms are included in the model of non-Newtonian flow, they can be treated by an algebraic solver in several ways. One option is to treat them explicitly and include them only in the residual part of (1.2). This would lead to the same linearized problem as before on every nonlinear iteration. Alternatively, one may linearize the inertia terms and include them in the definition of $\widetilde{F}(\mathbf{u}^{n-1}, p^{n-1})^{-1}$. In this case, (2.3) would correspond to the Oseen-type problem with variable viscosity. One may combine the techniques discussed in [12, 28] with the results of the present paper. The time-dependent case does not cause any additional difficulties. In general, it typically leads to a better-conditioned matrix $A$ and the pressure Schur complement preconditioner $\widehat{S}^{-1}$ should include an approximate pressure Poisson solve; cf. [7, 19].

*Remark* 7. Although in this paper we focus on applications in non-Newtonian fluid modeling, the preconditioning discussed here can be efficiently used in other fields where one has to solve (1.7) numerically. Numerical results for geophysical problems, such as magma migration and mantle convection, demonstrating the efficiency of such preconditioning, can be found in [6].

**4. Application to the Bingham problem.** Here we apply the analysis of the previous section to the regularized Bingham model of viscoplastic fluid. We will show that for a particular flow, when the norms of $\nu$ can be evaluated explicitly, the estimate of Lemma 3.4 provides a useful bound on the eigenvalues of the preconditioned operator. In the next section the effect of different preconditioning will be illustrated numerically.

Let $\Omega \in \mathbb{R}^d$, $d = 2, 3$ be a bounded connected domain. A slow and steady flow of the viscoplastic Bingham fluid is described by the following system of equations:

$$\begin{aligned} -\mathbf{div}\,\boldsymbol{\tau} + \nabla p &= \mathbf{f}, \\ \operatorname{div}\mathbf{u} &= 0, \\ \mathbf{u} &= \mathbf{u}_b \quad \text{on} \quad \partial\Omega \end{aligned} \tag{4.1}$$

and constitutive relations:

$$\begin{aligned} \boldsymbol{\tau} &= 2\mu\mathbf{D}\mathbf{u} + \tau_s \frac{\mathbf{D}\mathbf{u}}{|\mathbf{D}\mathbf{u}|} \quad \text{if} \quad |\mathbf{D}\mathbf{u}| \neq 0, \\ |\boldsymbol{\tau}| &\leq \tau_s \quad \text{if} \quad |\mathbf{D}\mathbf{u}| = 0, \end{aligned} \tag{4.2}$$

where $\mathbf{u}, p, \boldsymbol{\tau}$ are unknown velocity, pressure, and stress tensor, $\mu$ is a constant plastic viscosity, and $\tau_s$ is the yield stress. For $\tau_s = 0$ the system (4.1)–(4.2) reduces to the Stokes problem.

Copyright © by SIAM. Unauthorized reproduction of this article is prohibited.

If $\tau_s > 0$, the equations (4.1) are imposed only in the *flow region*, where $|\mathbf{Du}| > 0$, and make no sense in the *rigid region* $\Omega_r = \{\mathbf{x} \in \Omega \,|\, \mathbf{Du}(\mathbf{x}) = 0\}$. Both regions are a priori unknown. A common way to avoid this difficulty is to regularize (4.2); see, e.g., [3, 30]. Following [3], instead of (4.2) we set

$$\boldsymbol{\tau} = 2\mu\mathbf{Du} + \tau_s \frac{\mathbf{Du}}{\sqrt{\varepsilon^2 + |\mathbf{Du}|^2}} \tag{4.3}$$

for some small $\varepsilon > 0$. This enables us to consider the system of equations (4.1) and relations (4.3) in the whole computational domain and brings us to the model problem (1.2) with

$$\nu(|\mathbf{Du}|) = 2\mu + \frac{\tau_s}{\sqrt{\varepsilon^2 + |\mathbf{Du}(\mathbf{x})|^2}}.$$

For modeling reasons the parameter $\varepsilon$ should be small enough to ensure that the non-Newtonian fluid described by (4.1) and (4.3) well approximates the viscoplastic medium. The well-known result[2] [14] is

$$\|\nabla(\mathbf{u} - \mathbf{u}_\varepsilon)\| \le c\sqrt{\varepsilon}, \tag{4.4}$$

where $\mathbf{u}$ and $\mathbf{u}_\varepsilon$ are the solutions to the nonregularized ((4.1), (4.2)) and regularized ((4.1), (4.3)) problems, respectively. We will see that reasonably small (from the modeling point of view) values of $\varepsilon$ may lead to the serious loss of efficiency of linear and nonlinear iterative solvers. If we assume $\mathbf{u} \in W^{1,\infty}(\Omega)$, $\mu = O(1)$, and $\tau_s > 0$, then for the spectrum bounds in (3.1) we have $c_0^2 \nu_{\max}^{-1} = O(\varepsilon)$, $\nu_{\min}^{-1} = O(1)$. This leads to the following estimate of the condition number:

$$\operatorname{cond}(M^{-1}S) \le c\,\frac{1}{\varepsilon}. \tag{4.5}$$

Indeed, numerical experiments in section 5 show that the bound (4.5) is sharp with respect to $\varepsilon$ and the convergence of a Krylov subspace solver with block preconditioner (2.4) and $\widehat{S} = M$ seriously deteriorates for small $\varepsilon$. The same experiments show that the preconditioning with $M_\nu$ leads to significantly better convergence. To explain this numerical observation we consider an analytical solution to the Bingham problem and evaluate the constant $\tilde{c}_\nu$ given by Lemma 3.4.

Unlike the Stokes case, not a lot of reasonable analytical solutions are known for the Bingham problem. One is the flow between two planes: $\mathbf{u} = (u, v, w)$ with

$$\begin{aligned} u &= \begin{cases} \frac{1}{8}(1-2\tau_s)^2 & \text{if } \frac{1}{2} - \tau_s \le y \le \frac{1}{2} + \tau_s, \\ \frac{1}{8}\left[(1-2\tau_s)^2 - (1-2\tau_s-2y)^2\right] & \text{if } 0 \le y < \frac{1}{2} - \tau_s, \\ \frac{1}{8}\left[(1-2\tau_s)^2 - (2y-2\tau_s-1)^2\right] & \text{if } 1 \ge y > \frac{1}{2} + \tau_s, \end{cases} \\ v &= w = 0, \\ p &= -x. \end{aligned} \tag{4.6}$$

The rigid region consists of a constantly moving kernel for $\frac{1}{2} - \tau_s \le y \le \frac{1}{2} + \tau_s$. The yield stress $\tau_s = 0.5$ is the critical value, when the flow region disappears. The

[2] Although the best currently known for a general Bingham flow, the result is likely nonoptimal in terms of $\varepsilon$ [15].

Copyright © by SIAM. Unauthorized reproduction of this article is prohibited.

solution can be considered in the three-dimensional as well as in the two-dimensional case.

Let $\Omega = (0,1)^d$. For the constant $\tilde{c}_\nu$ given by Lemma 3.3, one easily finds $\tilde{c}_\nu = O(\varepsilon)$. This result gives no improvement over (4.5). However, we benefit from the natural decomposition of $\Omega$ into flow and rigid regions and we apply Lemma 3.4. To this end, we set $\Omega_1$ equal to the rigid zone; $\Omega_2$ and $\Omega_3$ are two flow regions given by $0 < y < \frac{1}{2} - \tau_s$ and $1 > y > \frac{1}{2} + \tau_s$, respectively. Since $\nu = \text{const} > 0$ in $\Omega_1$, we get $\nabla \nu^{-\frac{1}{2}} = 0$ in $\Omega_1$ and $\tilde{c}_\nu(\Omega_1) = O(1)$. In $\Omega_2$ one finds by the straightforward computations $\|\nabla \nu^{-\frac{1}{2}}\|_{L^\infty(\Omega_2)} = O(1)$ and $\|\nu^{\frac{1}{2}}\|_{L^k(\Omega_2)} = O(\varepsilon^{\frac{2-k}{2k}})$ for $k > 2$. The same relations hold for $\Omega_3$. Therefore we get, for the constant $\tilde{c}_\nu$ given by Lemma 3.4, $\tilde{c}_\nu \geq c(s)\varepsilon^{-s}$ for any $s > 0$ in the two-dimensional case and $\tilde{c}_\nu \geq c\,\varepsilon^{-\frac{1}{3}}$ in the three-dimensional case. If we assume that similar estimates are enjoyed by the constant from the discrete counterpart of (3.11), then due to (3.28) we get

$$\begin{aligned} &d = 2: \quad \lambda_{\max}(M_\nu^{-1}S)/\lambda_7(M_\nu^{-1}S) \leq c(s)\,\varepsilon^{-s} \qquad \forall\ s > 0, \\ &d = 3: \quad \lambda_{\max}(M_\nu^{-1}S)/\lambda_7(M_\nu^{-1}S) \leq c\,\varepsilon^{-\frac{1}{3}}. \end{aligned} \tag{4.7}$$

Comparing to (4.5), we see that the simple preconditioning with $M_\nu$ ameliorates much of the bad scaling of the condition number with respect to $\varepsilon$. The influence of $\lambda_n$, $n = 2, \ldots, 6$ on the convergence of a Krylov subspace method would be neutralized by at most five additional iterations.

Finally, we note that regularized models different from (4.3) (e.g., from [30]) can be considered in the same way.

**5. Numerical results.** In this section we show results of several numerical experiments for the equations of the regularized Bingham model. The goal of these experiments is to test the preconditioners discussed in section 2 and to verify whether the analysis from sections 3 and 4 is predictive. To run the numerical experiments we use two different discretizations. One is given by the FE method (2.2) with isoP2-P1 elements for the velocity-pressure spaces $\mathbb{V}_h$–$\mathbb{Q}_h$. This pair of spaces satisfies the LBB condition (2.1). Another is the extension of the well-known MAC FD scheme [13] for the case of non-Newtonian flows as described in [23]. Both discretizations use the uniform grid with mesh-size $h$.

**5.1. Linearized problem.** First we consider in $\Omega = (0,1)^2$ the linearized problem (1.7) with

$$\nu(\mathbf{x}) = \nu(|\mathbf{Du}(\mathbf{x})|) = 2\mu + \frac{\tau_s}{\sqrt{\varepsilon^2 + |\mathbf{Du}(\mathbf{x})|^2}},$$

where the velocity vector field $\mathbf{u}$ is known and given by (4.6). We fix $\mu = 1$, $\tau_s = 0.3$, and we vary the regularization parameter $\varepsilon$. Both FD and FE discretizations lead to the saddle–point-type system (2.3). For the FE method, the matrix $M$ is the pressure mass matrix, and $M_\nu$ is defined in (3.8). For finite differences, the corresponding choices are $M = I$ ($I$ is the identity matrix) and $M_\nu = \text{diag}(\nu^{-1}(\mathbf{x}_i))$; i.e., the $i$th main-diagonal element is equal to $\nu^{-1}(\mathbf{x}_i)$, where $\mathbf{x}_i$ denotes the grid node corresponding to the $i$th pressure degree of freedom.

Table 5.1 shows few minimal nonzero and maximal eigenvalues for $M^{-1}S$ and $M_\nu^{-1}S$ (recall that $\lambda_1 = 0$ in both cases). Figure 5.1 plots all eigenvalues for $\varepsilon = 10^{-3}$ and $\varepsilon = 10^{-5}$ and the FD discretization. For the FE discretization the eigenvalues' plots are not shown, since they are qualitatively similar to the FD case. We observe

Copyright © by SIAM. Unauthorized reproduction of this article is prohibited.

TABLE 5.1
*Eigenvalues of $M^{-1}S$ and $M_\nu^{-1}S$: FD with $h=\frac{1}{32}$ and FE with $h=\frac{1}{16}$; $\tau_s=0.3$.*

| $\varepsilon$ | $\lambda_2(M^{-1}S)$ | $\lambda_{\max}(M^{-1}S)$ | $\lambda_2(M_\nu^{-1}S)$ | $\lambda_3(M_\nu^{-1}S)$ | $\lambda_{\max}(M_\nu^{-1}S)$ |
|---|---|---|---|---|---|
| | MAC | | | | |
| 0.1 | 3.258e−1 | 0.284 | 3.428e−1 | 3.465e−1 | 1.042 |
| 0.01 | 7.982e−2 | 0.265 | 1.129e−1 | 1.129e−1 | 1.460 |
| 1e–3 | 8.705e−3 | 0.264 | 2.969e−2 | 3.457e−2 | 1.873 |
| 1e–4 | 8.783e−4 | 0.264 | 3.240e−3 | 2.526e−2 | 1.983 |
| 1e–5 | 8.791e−5 | 0.264 | 3.271e−4 | 2.427e−2 | 1.998 |
| | isoP2-P1 | | | | |
| 0.1 | 3.027e−2 | 0.233 | 1.116e−1 | 1.160e−1 | 1.010 |
| 0.01 | 1.385e−2 | 0.189 | 1.101e−1 | 1.109e−1 | 1.362 |
| 1e–3 | 1.470e−3 | 0.185 | 6.164e−2 | 6.208e−2 | 1.707 |
| 1e–4 | 1.480e−4 | 0.185 | 7.543e−3 | 4.456e−2 | 1.687 |
| 1e–5 | 1.481e−5 | 0.184 | 7.725e−4 | 4.260e−2 | 1.494 |

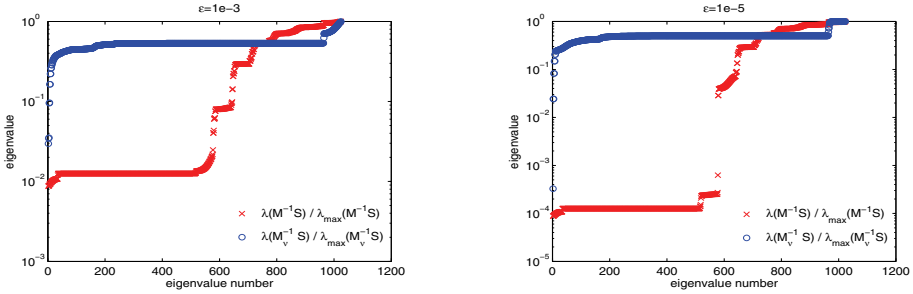


FIG. 5.1. *All nonzero eigenvalues for $\varepsilon=10^{-3}$ (left) and $\varepsilon=10^{-5}$ (right) for $h=\frac{1}{32}$ and $\tau_s=0.3$.*

the asymptotics

$$\begin{aligned}&\lambda_2(M^{-1}S)=O(\varepsilon),\quad \lambda_{\max}(M^{-1}S)=O(1)\qquad\text{and}\\ &\lambda_2(M_\nu^{-1}S)=O(\varepsilon),\quad \lambda_{\max}(M_\nu^{-1}S)=O(1).\end{aligned}\tag{5.1}$$

For other eigenvalues it clearly holds that

$$\lambda_k(M^{-1}S)=O(\varepsilon)\quad\text{for}\quad k=3,\dots K,\quad\text{with}\quad K\gg 1,\tag{5.2}$$

but

$$\lambda_k(M_\nu^{-1}S)=O(1)\quad\text{for}\quad k\geq 3.\tag{5.3}$$

Results in (5.1)–(5.3) agree very well with the theoretical eigenvalue bounds in (4.5) and (4.7) and the upper bounds given by Lemmas 3.1 and 3.2, suggesting that these bounds are almost sharp in terms of $\varepsilon$. In particular, the $\varepsilon$-dependence of the minimal nonzero eigenvalue of $M_\nu^{-1}S$ indicates that the lack of an estimate for the few smallest eigenvalues in (3.28) is not an artifact of the proof. Thus, for the present example our analysis predicts an almost $\varepsilon$-independent bound for $\lambda_7$, while experiments show that such a bound is likely to hold already for $\lambda_3$. From Figure 5.1 we see that the $\nu$-dependent preconditioner $M_\nu$ leads to a better clustering of the eigenvalues. This

Copyright © by SIAM. Unauthorized reproduction of this article is prohibited.

TABLE 5.2
*Eigenvalues of $\widehat{M}_\nu^{-1}M_\nu$ for the FE method with $h=\frac{1}{16}$ and $\tau_s=0.3$.*

| $\varepsilon$ | 0.1 | 0.01 | 1e−3 | 1e−4 | 1e−5 |
|---|---|---|---|---|---|
| $\lambda_1(\widehat{M}_\nu^{-1}M_\nu)$ | 0.500 | 0.499 | 0.498 | 0.498 | 0.497 |
| $\lambda_{\max}(\widehat{M}_\nu^{-1}M_\nu)$ | 2.000 | 2.002 | 2.004 | 2.004 | 2.005 |

property will be even more evident for the nonanalytical example in section 5.2.2 (see Figure 5.3).

For FE discretizations, one is also interested in having a simple approximation for the mass-type matrix $M_\nu$, since $M_\nu^{-1}$ is not a sparse matrix in contrast to the FD case. Table 5.2 shows that the diagonal matrix $\widehat{M}_\nu=\mathrm{diag}(M_\nu)$ is a very good approximation to $M_\nu$. Thus for the FE problem one can set $\widehat{S}=\widehat{M}_\nu$, or define $\widehat{S}^{-1}z$ through a fixed number of linear iterations for solving the system $\widehat{M}_\nu^{-1}M_\nu y=\widehat{M}_\nu^{-1}z$ with the zero initial guess [40].

**5.2. The Bingham problem.** Further, we solve numerically the nonlinear problem (4.1), (4.3) with Picard iterations (1.2). In section 5.3 we also consider the application of the Picard–Newton method. We will monitor the convergence of the linear and nonlinear solvers as well as the solution accuracy for different values of $\varepsilon$.

**5.2.1. Analytical test.** In this section we consider the regularized Bingham problem in a channel. For this problem we know the exact solution in the limit case of $\varepsilon=0$; i.e., $\mathbf{u}$ is given by (4.6). On every iteration of (1.2), the linearized problem (1.6) was solved by the MINRES iterative method with preconditioner (2.4). For $\widehat{A}$ we take the exact factorization for the (1,1)-submatrix $A$; the choice of $\widehat{S}$ was described in section 5.1. The accuracy is measured in the discrete $L^2$ norm for velocity and pressure:

$$err_u=\frac{\|\mathbf{u}-\mathbf{u}_h\|}{\|\mathbf{u}\|},\quad err_p=\frac{\|p-p_h\|_{L^2(\Omega_f)}}{\|p\|_{L^2(\Omega_f)}},$$

where $\Omega_f$ is the flow region, $\Omega_f=\Omega_2\cap\Omega_3$. Table 5.3 shows the discrete solution accuracy for different values of $\varepsilon$, the total number of Picard iterations, and the average number of the inner MINRES iterations. To calculate results from Table 5.3, we stop the outer Picard iterations when the $\ell_2$-norm of the nonlinear residual was less than $10^{-4}$ and the inner MINRES iterations were stopped once the $\ell_2$-norm of the initial residual has been reduced by at least five orders of magnitude. We note that setting such a tight inner tolerance is often not necessary in practice. The linearized problem on every nonlinear iteration can be solved with a lower accuracy. We will illustrate this option for the driven cavity test problem in the next section.

In agreement with our analysis, the choice of $\widehat{S}=M_\nu$ makes the performance of the linear iterations robust with respect to the parameter $\varepsilon$, while for the simple choice $\widehat{S}=M$, the number of inner iterations increases for $\varepsilon\to 0$. For the present example and given $h$ it does not make sense to decrease $\varepsilon$ below $10^{-4}$ or $10^{-5}$, since the discretization error begins to dominate over the modeling error. The velocity profiles of $u_h(\frac{1}{2},y)$ are shown in Figure 5.2 (with $h=\frac{1}{32}$, $\tau_s=0.3$ and varying $\varepsilon$).

**5.2.2. Driven cavity test.** The next test is the two-dimensional lid-driven cavity problem: $\Omega=(0,1)^2$, $\mathbf{f}=0$, with $\mathbf{u}(\mathbf{x})|_{y=1}=(1,0)$ and homogeneous Dirichlet

Copyright © by SIAM. Unauthorized reproduction of this article is prohibited.

TABLE 5.3
*Solution accuracy and iteration numbers for channel flow with $\tau_s = 0.3$, $h = \frac{1}{32}$ for the MAC discretization. Inner iterations' tolerance: $10^{-5}$.*

| | $\varepsilon$ | | | | |
|---|---|---|---|---|---|
| | 0.1 | 0.01 | 1e−3 | 1e−4 | 1e−5 |
| $err_u$ | 1.38e−1 | 3.77e−2 | 5.73e−3 | 1.53e−3 | 1.34e−3 |
| $err_p$ | 3.79e−1 | 1.33e−1 | 4.48e−2 | 2.30e−2 | 2.03e−2 |
| #Picard iter. | 10 | 24 | 51 | 61 | 81 |
| #linear iter. $\widehat{S} = M$ | 13.8 | 27.0 | 56.7 | 92.3 | 147 |
| #linear iter. $\widehat{S} = M_\nu$ | 13.7 | 19.8 | 25.8 | 26.5 | 25.9 |

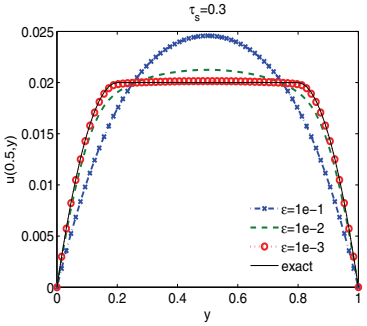


FIG. 5.2. *Velocity profiles of discrete solutions for different $\varepsilon$.*

TABLE 5.4
*Iteration numbers for driven cavity problem $h = \frac{1}{32}$ and varying $\varepsilon$. Inner iterations' tolerance: $10^{-2}$.*

| | MAC | | | | isoP2-P1 | | | |
|---|---|---|---|---|---|---|---|---|
| $\varepsilon$ | 0.1 | 0.01 | 1e−3 | 1e−4 | 0.1 | 0.01 | 1e−3 | 1e−4 |
| | $\tau_s = 2$ | | | | $\tau_s = 2$ | | | |
| #Picard iter. | 22 | 63 | 103 | 119 | 23 | 77 | 214 | 430 |
| #linear iter. $\widehat{S} = M$ | 8.8 | 12.3 | 22.8 | 46.1 | 4.9 | 7.6 | 10 | 30* |
| #linear iter. $\widehat{S} = M_\nu$ | 7.5 | 6.6 | 5.9 | 6.0 | 3.0 | 2.4 | 2.1 | 2.4 |
| | $\tau_s = 5$ | | | | $\tau_s = 5$ | | | |
| #Picard iter. | 34 | 81 | 117 | 127 | 37 | 118 | 287 | 454 |
| #linear iter. $\widehat{S} = M$ | 9.4 | 15.2 | 28.8 | 54.4 | 5.4 | 8.3 | 11.6 | 35* |
| #linear iter. $\widehat{S} = M_\nu$ | 7.4 | 7.2 | 6.6 | 6.4 | 2.3 | 2.3 | 2.3 | 2.1 |

boundary conditions on the rest of the boundary. The solution has a nonphysical singular behavior in the upper corners; however, the problem serves as a standard benchmark for incompressible CFD codes.

Tables 5.4 and 5.5 show the total number of Picard iterations and the average number of inner MINRES (or BiCGstab for isoP2-P1) iterations for different values of $\varepsilon$ and mesh sizes. To produce results from Tables 5.4 and 5.5, we take the solution of the Stokes problem ($\tau_s = 0$) as the initial guess and stop the outer Picard iterations when the $\ell_2$-norm of the nonlinear residual was reduced by at least the factor $10^5$. Unlike the previous test, the tolerance for the inner iterations was taken less tightly; i.e., the inner iterations were stopped once the $\ell_2$-norm of the initial residual had been reduced by $10^2$. Such weakening of the inner tolerance has almost no effect on the total

Copyright © by SIAM. Unauthorized reproduction of this article is prohibited.

TABLE 5.5

*Iteration numbers for driven cavity problem $\varepsilon = 1e-3$ and varying $h$. Inner iterations' tolerance: $10^{-2}$; isoP2-P1 elements.*

| $h$ | $\frac{1}{16}$ | $\frac{1}{32}$ | $\frac{1}{64}$ | $\frac{1}{128}$ | $\frac{1}{256}$ | $\frac{1}{16}$ | $\frac{1}{32}$ | $\frac{1}{64}$ | $\frac{1}{128}$ | $\frac{1}{256}$ |
|---|---|---|---|---|---|---|---|---|---|---|
| | $\tau_s = 2$ | | | | | $\tau_s = 5$ | | | | |
| #Picard iter. | 169 | 214 | 246 | 196 | 170 | 230 | 287 | 365 | 339 | 308 |
| #linear iter. $\widehat{S} = M_\nu$ | 2.2 | 2.1 | 2.0 | 2.1 | 2.1 | 2.4 | 2.3 | 2.2 | 2.3 | 2.3 |

TABLE 5.6

*Eigenvalues of $M^{-1}S$ and $M_\nu^{-1}S$ on the last Picard iteration for the driven cavity problem; isoP2-P1 with $h = \frac{1}{16}$ and $h = \frac{1}{28}$.*

| | $\tau_s = 2$ | | | | $\tau_s = 5$ | | | |
|---|---|---|---|---|---|---|---|---|
| $\varepsilon$ | 0.1 | 0.01 | 1e−3 | 1e−4 | 0.1 | 0.01 | 1e−3 | 1e−4 |
| $h = \frac{1}{16}$ | | | | | | | | |
| $\lambda_2(M^{-1}S)$ | 5.45e4−3 | 5.96e−4 | 6.02e−5 | 6.03e−6 | 2.30e−3 | 2.39e−4 | 2.34e−5 | 2.40e−6 |
| $\lambda_{\max}(M^{-1}S)$ | 0.377 | 0.376 | 0.376 | 0.376 | 0.307 | 0.306 | 0.306 | 0.306 |
| $\lambda_2(M_\nu^{-1}S)$ | 1.13e−1 | 1.12e−1 | 1.12e−1 | 1.12e−1 | 1.02e−1 | 9.83e−2 | 9.30e−2 | 9.14e−2 |
| $\lambda_{\max}(M_\nu^{-1}S)$ | 1.435 | 1.678 | 1.626 | 1.358 | 1.566 | 1.790 | 1.749 | 1.688 |
| $h = \frac{1}{28}$ | | | | | | | | |
| $\lambda_2(M^{-1}S)$ | 5.44e−3 | 5.93e−4 | 5.98e−5 | 5.99e−6 | 2.30e−3 | 2.38e−4 | 2.39e−5 | 2.39e−6 |
| $\lambda_{\max}(M^{-1}S)$ | 0.409 | 0.408 | 0.408 | 0.408 | 0.351 | 0.350 | 0.350 | 0.350 |
| $\lambda_2(M_\nu^{-1}S)$ | 1.16e−1 | 1.15e−1 | 1.15e−1 | 1.15e−1 | 1.09e−1 | 1.06e−1 | 1.02e−1 | 1.00e−1 |
| $\lambda_{\max}(M_\nu^{-1}S)$ | 1.487 | 1.799 | 1.814 | 1.690 | 1.622 | 1.860 | 1.893 | 1.882 |

number of the outer iterations (the exceptions are marked by asterisks in Table 5.4; here the stopping criteria was tightened to $10^{-3}$, otherwise the outer iterations (1.2) do not converge); the same observation is reported in [18]. Similar to the analytical test, the choice of $\widehat{S} = M_\nu$ makes the performance of the linear iterations robust with respect to the parameter $\varepsilon$ and the mesh size, while for the simple choice $\widehat{S} = M$ the number of inner iterations increases for $\varepsilon \to 0$. We recall that for the FE discretization we use the BiCGstab inner solver with triangular preconditioner (2.5). One iteration of BiCGstab is approximately twice as expensive as one iteration of MINRES.

Furthermore, we look for the eigenvalues' distribution of $M^{-1}S$ and $M_\nu^{-1}S$. Thus, Table 5.6 shows minimal nonzero and maximal eigenvalues for $M^{-1}S$ and $M_\nu^{-1}S$ ($\lambda_1 = 0$ in both cases) for several values of $\varepsilon$ and two levels of refinement. Figure 5.3 plots all eigenvalues for $\varepsilon = 10^{-3}$ and $\varepsilon = 10^{-4}$ and two values of the stress yield $\tau_s$. Again we observe that $\lambda_2(M^{-1}S) = O(\varepsilon)$ and $\lambda_{\max}(M^{-1}S) = O(1)$. With the new preconditioner, both the second and the maximal eigenvalues of $M_\nu^{-1}S$ are uniformly bounded with respect to $\varepsilon$.

From the modeling point of view the most challenging task is finding the rigid regions of the viscoplastic fluid flow. Formally, these are the regions where $\mathbf{D}\mathbf{u}_h = 0$. The latter condition, however, does not hold exactly for the numerical solution, especially if a regularized model is used. For the driven cavity problem, some numerical results, including the prediction of the rigid zones, can be found in [10, 11, 22, 26, 38]. In [22, 11], a regularized model was used, while [10, 26, 38] considered the nonregularized Bingham model. To give an insight into the quality of the discrete solution for different values of the regularization parameter $\varepsilon$, Figures 5.4 and 5.5 show computed

Copyright © by SIAM. Unauthorized reproduction of this article is prohibited.

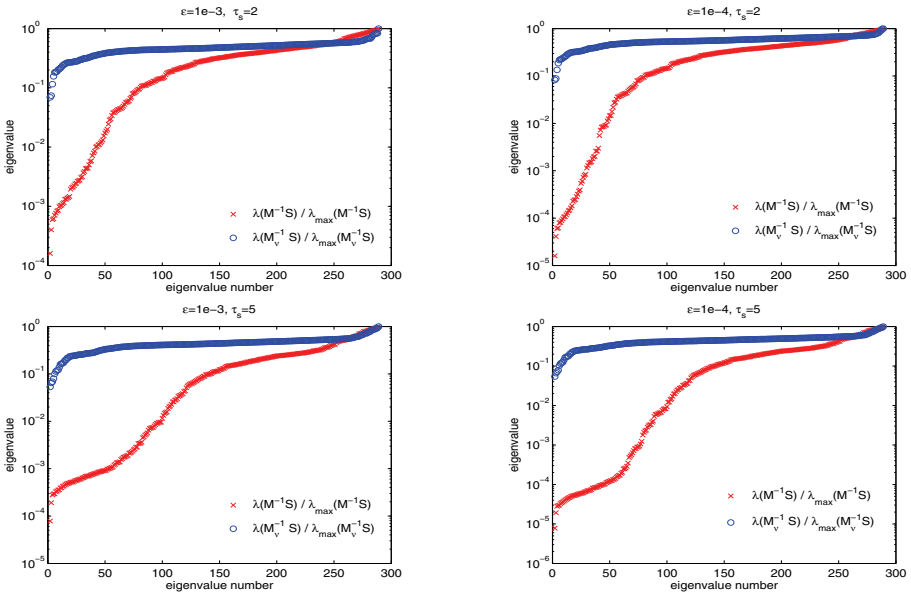


FIG. 5.3. *All (scaled) nonzero eigenvalues on the last Picard iteration for the driven cavity problem with* $\tau = 2$ *(top) and* $\tau = 5$ *(bottom), and* $\varepsilon = 10^{-3}$ *(left) and* $\varepsilon = 10^{-4}$ *(right); isoP2-P1 with* $h = \frac{1}{16}$.

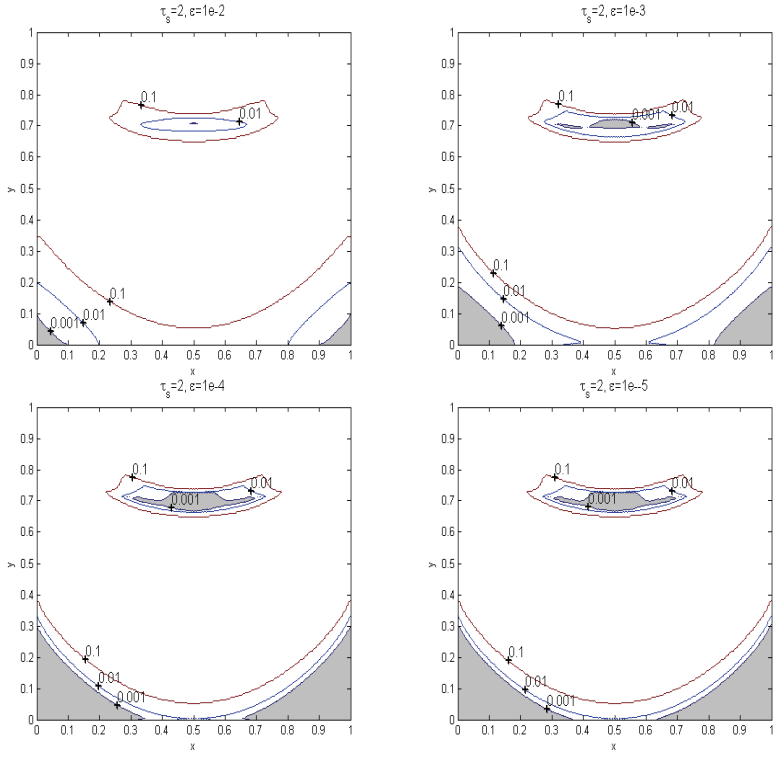


FIG. 5.4. *Approximation of the rigid zones for the driven cavity problem with* $\tau_s = 2$ *and varying* $\varepsilon$*; isolines for* $|\mathbf{Du}_h|$ *with values* $= \{10^{-1}, 10^{-2}, 10^{-3}\}$.

Copyright © by SIAM. Unauthorized reproduction of this article is prohibited.

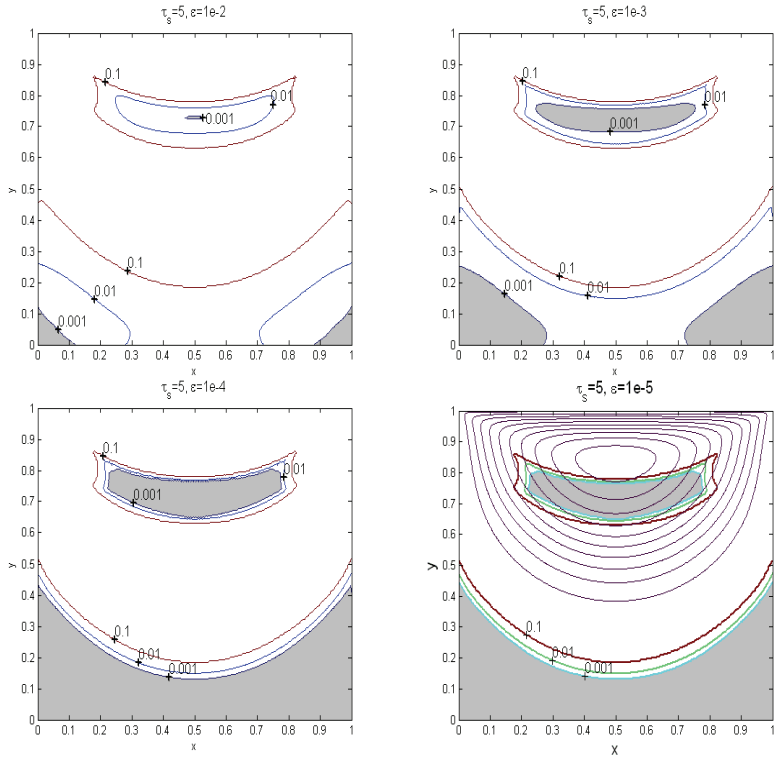


FIG. 5.5. *Approximation of the rigid zones for the driven cavity problem with* $\tau_s = 5$ *and varying* $\varepsilon$*; isolines for* $|\mathbf{D}\mathbf{u}_h|$ *with values* $= \{10^{-1}, 10^{-2}, 10^{-3}\}$ *and equally-distant streamlines for* $\varepsilon = 1e-5$.

isolines of $|\mathbf{D}\mathbf{u}_h|$ for $\varepsilon \in \{10^{-2}, 10^{-3}, 10^{-4}, 10^{-5}\}$. We plot the isolines with the values $\{10^{-1}, 10^{-2}, 10^{-3}\}$ and shadow the regions where $|\mathbf{D}\mathbf{u}_h| \le 10^{-3}$. From these results and the results of the papers cited above, it follows that for $\varepsilon \lesssim 10^{-4}$ the shadowed region gives a fairly good prediction of a rigid zone. At the same time, the values of the regularization parameter $\varepsilon \gtrsim 10^{-3}$ are not small enough to recover the viscoplastic behavior of fluid. Note that the sufficiently small (from the modeling point of view) values of $\varepsilon$ are those values when the developed preconditioner $M_\nu$ gives a significant improvement of the linear solver performance.

**5.3. On Picard–Newton iterations.** Results in Tables 5.3 and 5.4 show that for small $\varepsilon$ the number of outer nonlinear iterations increases. To improve the situation one might consider Newton-type methods instead of the Picard iterations. As discussed in Remark 4, this would lead to a more complicated linear algebraic system to be solved on each nonlinear iteration. However, a fast convergence may overcompensate for a reduction in the linear inner solver efficiency. Unfortunately, as was noted already in [9] (see also numerical results in [18]), the Newton method for the regularized Bingham problem is not robust with respect to $\varepsilon$: the domain of convergence for the method shrinks as $\varepsilon \to 0$. Indeed, the norm of the matrix of the second derivatives grows as $O(\varepsilon^{-1})$ [9], implying that, to ensure convergence, the initial guess for the Newton method should belong to an $O(\varepsilon)$-neighborhood of the (unknown) solution. There are several ways to make use of the Newton method in such a situation. One possibility is to combine it with the continuation method

Copyright © by SIAM. Unauthorized reproduction of this article is prohibited.

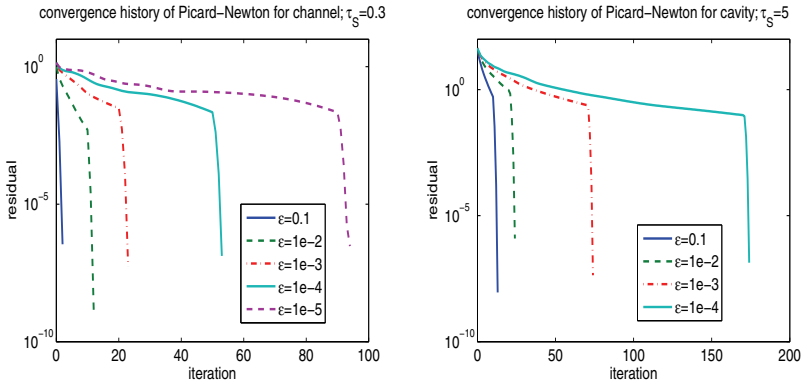


FIG. 5.6. *Convergence histories of the Picard–Newton method for the channel problem with* $\tau_s = 0.3$ *and the driven cavity problem with* $\tau_s = 5$ *and varying* $\varepsilon$*; isoP2-P1 FE with* $h = \frac{1}{32}$.

in $\varepsilon$. Another option is to perform a number of Picard iterations and switch to the Newton method when a sufficiently good approximation to the solution is found. We explore numerically the second approach, which we call the Picard–Newton iteration. Convergence histories of the method for the channel and the driven cavity problems are shown in Figure 5.6. For every ten Picard steps we perform one Newton iteration; if this Newton iteration decreases the residual, we accept the new approximation and switch to the Newton iteration; otherwise, the new approximation is declined and we continue with the Picard method. Obviously, with the decreasing of $\varepsilon$ one needs more Picard steps to get a satisfactory initial guess for the Newton method. Nevertheless, comparing the results with those for the pure Picard method in Table 5.4, we note that the total number of the outer iterations decreases by a factor of 3–5. Once the good approximation is obtained, the Newton method converges very fast (2–3 iterations). Thus the majority of the computation time in such an approach is still spent by the Picard iteration.

**6. Conclusions.** The paper presents a new preconditioning technique for FE discretizations of the Stokes-type problem with variable viscosity. The preconditioner is block diagonal or block triangular and requires an efficient approximate solver for the (1,1)-block and a preconditioner for the Schur complement of the system. One can use standard sparse solvers for the (1,1)-block. For the Schur complement preconditioning, we suggest using a mass-type matrix with respect to a viscosity-dependent weighted $L^2$ scalar product and a special diagonal matrix for FE or FD approximations, respectively. Theoretical analysis of the preconditioner is based on the weighted Nečas inequality. We have proved some bounds for the best constant in the weighted Nečas inequality, which depend on some norms of the viscosity coefficient and the gradient of its inverse. We have applied the preconditioning and its analysis to the linearized equations of the regularized Bingham model of viscoplastic fluid. For this application we have shown that the preconditioner is efficient, and the analytical bounds are useful and predictive. In particular, numerical examples demonstrate the robustness of the preconditioner with respect to the variation of mesh size and the regularization parameter of the fluid model. It was observed that for those values of the regularization parameter where the viscoplastic behavior of the fluid is recovered, the use of the special viscosity-dependent preconditioning becomes inevitable. An $\varepsilon$-insensitive nonlinear iterative method for the regularized Bingham model is still

Copyright © by SIAM. Unauthorized reproduction of this article is prohibited.

an issue. We have shown that the Picard iteration can be enhanced by the Newton method to considerably reduce the number of nonlinear iterations for the small values of the regularization parameter.

Finally, we mention that while in this paper we have focused on the applications in non-Newtonian fluid modeling, the approach is efficient for solving the variable viscosity Stokes-type problems arising in other areas, e.g., in geophysical fluids modeling.

## REFERENCES


[1] R. Bank, B. D. Welfert, and H. Yserentant, *A class of iterative methods for solving saddle point problems*, Numer. Math., 56 (1990), pp. 645–666.

[2] M. Benzi, G. H. Golub, and J. Liesen, *Numerical solution of saddle point problems*, Acta Numer., 14 (2005), pp. 1–137.

[3] M. Bercovier and M. Engelman, *A finite element method for incompressible non-Newtonian flows*, J. Comput. Phys., 36 (1980), pp. 313–326.

[4] J. Bramble and J. Pasciak, *A preconditioning technique for indefinite systems resulting from mixed approximation of elliptic problems*, Math. Comp., 50 (1988), pp. 1–17.

[5] F. Brezzi and M. Fortin, *Mixed and Hybrid Finite Element Methods*, Springer-Verlag, New York, 1991.

[6] C. Burstedde, O. Ghattas, G. Stadler, T. Tu, and L. C. Wilcox, *Parallel scalable adjoint-based adaptive solution of variable-viscosity Stokes flow problems*, Comput. Methods Appl. Mech. Engrg., 198 (2009), pp. 1691–1700.

[7] J. Cahouet and J. P. Chabard, *Some fast 3D finite element solvers for the generalized Stokes problem*, Internat. J. Numer. Methods Fluids, 8 (1988), pp. 869–895.

[8] U. Christensen and H. Harder, *3-D convection with variable viscosity*, Geophys. J. Internat., 104 (2007), pp. 213–220.

[9] E. J. Dean and R. Glowinski, *Operator-splitting methods for the simulation of Bingham visco-plastic flow*, Chinese Ann. Math. Ser. B, 23 (2002), pp. 187–204.

[10] E. J. Dean, R. Glowinski, and G. Guidoboni, *On the numerical simulation of Bingham visco-plastic flow: Old and new results*, J. Non-Newtonian Fluid Mech., 142 (2007), pp. 36–62.

[11] R. N. Elias, M. A. D. Martins, and A. L. G. A. Coutinho, *Parallel edge-based solution of viscoplastic flows with the SUPG/PSPG formulation*, Comput. Mech., 38 (2006), pp. 365–381.

[12] H. C. Elman, D. J. Silvester, and A. J. Wathen, *Finite Elements and Fast Iterative Solvers: With Applications in Incompressible Fluid Dynamics*, Numer. Math. Sci. Comput., Oxford University Press, New York, 2005.

[13] C. A. J. Fletcher, *Computational Techniques for Fluid Dynamics*, Springer-Verlag, Sydney, 1990.

[14] R. Glowinski, *Numerical Methods for Nonlinear Variational Problems*, Springer-Verlag, New York, 1984.

[15] R. Glowinski, *private communication*.

[16] W. Hackbusch, *Multi-grid Methods and Applications*, Springer-Verlag, Berlin, Heidelberg, 1985.

[17] J. Hron, J. Málek, J. Nečas, and K. R. Rajagopal, *Numerical simulations and global existence of solutions of two-dimensional flows of fluids with pressure- and shear-dependent viscosities*, Math. Comput. Simulation, 61 (2003), pp. 297–315.

[18] J. Hron, A. Ouazzi, and S. Turek, *A Computational Comparison of two FEM Solvers for Nonlinear Incompressible Flow*, in Challenges in Scientific Computing, Lect. Notes Comput. Sci. Eng. 35, Springer-Verlag, Berlin, 2003.

[19] G. M. Kobelkov and M. A. Olshanskii, *Effective preconditioning of Uzawa type schemes for generalized Stokes problem*, Numer. Math., 86 (2000), pp. 443–470.

[20] O. A. Ladyzhenskaya, *The Mathematical Theory of Viscous Incompressible Flows*, Gordon and Breach, London, 1969.

[21] J. Málek, J. Nečas, and K. R. Rajagopal, *Global existence of solutions for flows of fluids with pressure and shear dependent viscosities*, Appl. Math. Lett., 15 (2002), pp. 961–967.

[22] E. Mitsoulis and Th. Zisis, *Flow of Bingham plastics in a lid-driven cavity*, J. Non-Newtonian Fluid Mech., 101 (2001), pp. 173–180.

[23] E. A. Muravleva and M. A. Olshanskii, *Two finite-difference schemes for the Bingham cavity flows*, Russian J. Numer. Anal. Math. Modelling, 23 (2008), pp. 615–634.


Copyright © by SIAM. Unauthorized reproduction of this article is prohibited.

[24] J. Nečas, *Les Méthodes Directes en Théorie des Équations Elliptiques*, Masson, Paris, 1967.
[25] M. A. Olshanskii, *Lections and Exercises in Multigrid Methods*, Fizmatlit, Moscow, 2005.
[26] M. A. Olshanskii, *Analysis of semi-staggered finite-difference method with application to Bingham flows*, Comput. Methods Appl. Mech. Engrg., 198 (2009), pp. 975–985.
[27] M. A. Olshanskii and A. Reusken, *Analysis of a Stokes interface problem*, Numer. Math., 103 (2006), pp. 129–149.
[28] M. A. Olshanskii and Yu. V. Vassilevski, *Pressure Schur complement preconditioners for the discrete Oseen problem*, SIAM J. Sci. Comput., 29 (2007), pp. 2686–2704.
[29] A. Ouazzi, S. Turek, and J. Hron, *Finite element methods for the simulation of incompressible powder flow*, Comm. Numer. Methods Engrg., 21 (2005), pp. 581–596.
[30] T. C. Papanastasiou, *Flows of materials with yield*, J. Rheol., 31 (1987), pp. 385–404.
[31] A. Quarteroni and A. Valli, *Domain Decomposition Methods for Partial Differential Equations*, Numer. Math. Sci. Comput., Oxford University Press, New York, 1999.
[32] Y. Saad, *Iterative Methods for Sparse Linear Systems*, 2nd ed., SIAM, Philadelphia, 2003.
[33] D. Silvester and A. Wathen, *Fast iterative solution of stabilised Stokes systems Part* II: *Using general block preconditioners*, SIAM J. Numer. Anal., 31 (1994), pp. 1352–1367.
[34] J. W. Ruge and K. Stüben, *Algebraic Multigrid*, in Multigrid Methods, Frontiers Appl. Math., 3, SIAM, Philadelphia, 1987.
[35] P. J. Tackley, *Effects of strongly variable viscosity on three-dimensional compressible convection in planetary mantles*, J. Geophys. Res., 101 (1996), pp. 3311–3332.
[36] R. Temam, *Navier-Stokes Equations: Theory and Numerical Analysis*, Stud. Math. Appl., 2, North–Holland, Amsterdam, New York, 1979.
[37] H. Tennekes and J. L. Lumley, *A First Course in Turbulence*, MIT Press, Cambridge, MA, 1972.
[38] D. Vola, L Boscardin, and J. C. Latché, *Laminar unsteady flows of Bingham fluids: A numerical strategy and some benchmark results*, J. Comput. Phys., 187 (2003), pp. 441–456.
[39] A. J. Wathen, *Realistic eigenvalue bounds for the Galerkin mass matrix*, IMA J. Numer. Anal., 7 (1987), pp. 449–457.
[40] A. J. Wathen and T. Rees, *Chebyshev semi-iteration in preconditioning*, Electron. Trans. Numer. Anal., 34 (2009), pp. 125–135.

Copyright © by SIAM. Unauthorized reproduction of this article is prohibited.